Published in final edited form as:
Cancer Res. 2013 October 1; 73(19): 5985–5995. doi:10.1158/0008-5472.CAN-13-0755.

Chemoprevention of Prostate Cancer by D,L-Sulforaphane Is Augmented by Pharmacological Inhibition of Autophagy

Avani R. Vyas[1], **Eun-Ryeong Hahm**[1], **Julie A. Arlotti**[2], **Simon Watkins**[3], **Donna Beer Stolz**[3], **Dhimant Desai**[4], **Shantu Amin**[4], and **Shivendra V. Singh**[1,2]

[1]Department of Pharmacology & Chemical Biology, University of Pittsburgh School of Medicine, Pittsburgh, Pennsylvania

[2]University of Pittsburgh Cancer Institute, University of Pittsburgh School of Medicine, Pittsburgh, Pennsylvania

[3]Department of Cell Biology and Physiology, University of Pittsburgh School of Medicine, Pittsburgh, Pennsylvania

[4]Department of Pharmacology, Penn State Milton S. Hershey Medical Center, Hershey, Pennsylvania

Abstract

There is preclinical evidence that oral administration of D,L-sulforaphane (SFN) can decrease the incidence or burden of early-stage prostate cancer (PIN) and well-differentiated cancer (WDC), but not late-stage poorly differentiated cancer (PDC). Because SFN treatment induces cytoprotective autophagy in cultured human prostate cancer cells, the present study tested the hypothesis that chemopreventive efficacy of SFN could be augmented by pharmacological inhibition of autophagy using chloroquine (CQ). Incidence of PDC characterized by prostate weight of >1g was significantly lower in the SFN+CQ group compared with control (P=0.004), CQ (P=0.026) or SFN group (P=0.002 by Fisher's exact test). Average size of the metastatic lymph-node was lower by about 42% in the SFN+CQ group compared with control (P=0.043 by Wilcoxon test). On the other hand, the SFN+CQ combination was not superior to SFN alone with respect to inhibition of incidence or burden of microscopic PIN or WDC. SFN treatment caused *in vivo* autophagy as evidenced by transmission electron microscopy. Mechanistic studies showed that prevention of prostate cancer and metastasis by the SFN+CQ was associated with decreased cell proliferation, increased apoptosis, alterations in protein levels of autophagy regulators Atg5 and phospho-mTOR, and suppression of biochemical features of epithelial-mesenchymal transition. Plasma proteomics identified protein expression signature that may serve as biomarker

Correspondence to: Shivendra V. Singh, 2.32A Hillman Cancer Center Research Pavilion, University of Pittsburgh Cancer Institute, 5117 Centre Avenue, Pittsburgh, PA 15213. Phone: 412-623-3263; Fax: 412-623-7828; singhs@upmc.edu.

Conflict of Interest: None

Disclosure of Potential Conflicts of Interest:
No potential conflicts of interests were disclosed.

Authors' Contributions
Conception and design: S.V. Singh
Development of methodology: E.R. Hahm, D. Desai, S. Amin
Acquisition of data (provided animals, acquired and managed patients, provided facilities, etc.): A.R. Vyas, E.R. Hahm, J.A. Arlotti
Analysis and interpretation of data (e.g., statistical analysis, biostatistics, computational analysis): A.R. Vyas, E.R. Hahm, J.A. Arlotti, S.V. Singh
Writing, review and/or revision of the manuscript: A.R. Vyas, E.R. Hahm, S.V. Singh
Study supervision: S.V. Singh

of SFN+CQ exposure/response. This study offers a novel combination regimen for future clinical investigations for prevention of prostate cancer in humans.

Keywords

Sulforaphane; Autophagy; Prostate Cancer; Chemoprevention

Introduction

Cruciferous vegetable intake in the diet is inversely associated with the risk of different malignancies including cancer of the prostate (1,2), which is a leading cause of cancer-related deaths among men in the United States (3). Phytochemicals capable of eliciting cancer protective effect have now been isolated from different edible cruciferous vegetables including broccoli, watercress, and garden cress (4,5). Sulforaphane [1-isothiocyanato-4-(methylsulfinyl)-butane] is one such small molecule of interest for prevention of cancers (5). Sulforaphane (SFN) occurs naturally as a L-isomer, but its synthetic D,L-analogue has been studied extensively for cancer prevention properties (4,5). Naturally occurring or synthetic SFN has exhibited cancer chemopreventive effects in chemically-induced as well as oncogene-driven rodent cancer models (6–10). Talalay and co-workers were the first to report SFN-mediated inhibition of 9,10-dimethyl-1,2-benzanthracene-induced mammary cancer development in rats (6). Chemopreventive efficacy of SFN was subsequently established in other chemically-induced rodent cancer models, including tobacco-carcinogen-induced lung cancer (7), benzo[a]pyrene-induced stomach cancer (8), and azoxymethane-induced colonic aberrant crypt foci (9). Previous work from our own laboratory has revealed that oral administration of 6 μmol SFN three times per week results in significant inhibition of early-stage prostate carcinogenesis in Transgenic Adenocarcinoma of Mouse Prostate (TRAMP) mice without any side effects (10). Specifically, the incidence of prostatic intraepithelial neoplasia (PIN) and well-differentiated prostate cancer (WDC) were about 23–28% lower in the prostate of SFN-treated TRAMP mice compared with controls (10). However, the incidence of poorly-differential prostate cancer (PDC) was not affected by the SFN regimen employed in our study (10). In another study, feeding of TRAMP mice with 240 mg of broccoli sprout/day resulted in a significant decrease in prostate tumor growth (11). We were the first to demonstrate *in vivo* efficacy of SFN against PC-3 human prostate cancer xenografts in male athymic mice (12).

Insight into the mechanisms by which SFN likely prevents cancer development continues to expand, albeit mostly from cellular studies. Nevertheless, the mechanisms potentially contributing to SFN-mediated chemoprevention include cell cycle arrest (13), apoptosis induction (14,15), inhibition of angiogenesis and histone deacetylase (16,17), and suppression of oncogenic signaling pathways (eg, nuclear factor-κB, signal transducer and activator of transcription 3, and androgen receptor) (18–20). SFN is not a targeted agent as is the case for many other dietary cancer chemopreventive agents (21).

Previously, we made an exciting observation that exposure of cultured human prostate cancer cells (LNCaP and PC-3) to SFN resulted in induction of autophagy (22), which is an evolutionary conserved physiological process for bulk-degradation of macromolecules including organelles and considered a valid cancer therapeutic target (23,24). We also found that autophagy was a protective mechanism against apoptosis induction by SFN (22). However, the *in vivo* significance of these observations was unclear. The present study addresses this gap in our knowledge using autophagy inhibitor chloroquine (CQ) and the TRAMP mouse model of prostate cancer.

Materials and Methods

Reagents and antibodies

SFN was synthesized as described previously (7). The purity of SFN was 98% as determined by high-performance liquid chromatography. Stock solution of SFN was stored at −20°C. SFN was diluted with phosphate-buffered saline (PBS) immediately before use. CQ was purchased from Sigma-Aldrich. Antibodies against T-antigen, synaptophysin, and E-cadherin were from BD Biosciences; antibodies against microtubule-associated protein 1 light chain 3 (LC3), androgen receptor (AR), and vimentin were purchased from Santa Cruz Biotechnology; anti-Ki-67 antibody was purchased from Dako-Agilent Technologies; and antibodies against p62, cleaved caspase-3, Atg5 and phospho-(S2448)-mTOR were purchased from Cell Signaling Technology. Terminal deoxynucleotidyl transferase-mediated dUTP nick end labeling (TUNEL) staining was performed using ApopTag Plus Peroxidase *In Situ* Apoptosis Detection kit (EMD Millipore). A kit for quantitation of vascular endothelial growth factor (VEGF) in tumor lysates was purchased from R&D Systems.

Randomization and treatment of mice

Use of mice and their care were in accordance with the University of Pittsburgh Institutional Animal Care and Use Committee guidelines. Male TRAMP [(C57BL/6 FVB) F1] mice were obtained by crossing TRAMP female in the C57BL/6 background with male FVB mice. Transgene verification was performed as described by Greenberg et al. (25). After transgene verification, 4-week old male TRAMP mice were placed on AIN-93G diet (Harlan Teklad) for 1 week prior to the onset of treatments, and the mice were maintained on this diet throughout the experiment. Initially, as the mice became available from our breeding program, a total of 128 mice were placed into one of the following groups: control (n=32), CQ alone (n=32), SFN alone (n=35), and SFN+CQ combination (n=29). As summarized in Supplementary Table S1, some mice from each group were removed from the study due to a variety of reasons, including weight loss, hind limb paralysis, seminal vesicle invasion, and tumors at sites other than prostate. Final number of mice available for evaluations was: control (n=28), CQ alone (n=25), SFN alone (n=28), and SFN + CQ (n=25). Majority of the evaluable mice in each group were treated for 18 weeks but a fraction of mice from control (25%), CQ alone (16%), SFN alone (21%), and SFN+CQ combination group (8%) were sacrificed after 15–17 weeks of treatment due to large tumor burden. Nevertheless, these mice were included in the analysis. The mice of the control group received 0.1 mL PBS by oral intubation as well as intraperitoneal injection 3 times per week. The CQ alone group of mice were treated with 1.2 mg CQ (in 0.1 mL PBS) by intraperitoneal injection and 0.1 mL PBS by oral intubation 3 times per week. The SFN group of mice received 1 mg SFN (in 0.1 mL PBS) by oral intubation and 0.1 mL PBS by intraperitoneal injection 3 times per week. The SFN+CQ group of mice received 1 mg SFN (in 0.1 mL PBS) by oral intubation and 1.2 mg CQ (in 0.1 mL PBS) by intraperitoneal injection 3 times per week. Treatments were given on Monday, Wednesday, and Friday of each week. Body weights of the mice were recorded once weekly beginning at 5 weeks of age. The animals were sacrificed by CO_2 inhalation followed by cervical dislocation. Blood was collected for separation of plasma, which was stored at −20°C. The prostate tissues were harvested, weighed, fixed in 10% neutral-buffered formalin, and sectioned at 4–5 μm thickness.

Histopathological evaluations

Whole mount hematoxylin and eosin (H&E)-stained sections of prostate tissues were digitized by scanning and each section was blindly scored for microscopic PIN and WDC incidence and burden (affected area). The area of the lesions (in 2 dimensions) was calculated on histological slides using on-screen drawing tool of the WebScope viewing

software from Aperio. The mean PIN and WDC area were calculated from sum of the area in an animal and the average of area over all the animals for each group. Pathologic grading was consistent with the criteria defined in our previous studies (10,26).

Immunohistochemistry

Briefly, prostate sections were quenched with 3% hydrogen peroxide and blocked with normal serum. The sections were then probed with the desired primary antibody (anti-synaptophysin, anti-T-antigen, anti-Ki-67, anti-LC3, anti-AR), washed with tris-buffered saline and incubated with secondary antibody. Characteristic brown color was developed by incubation with 3,3′-diaminobenzidine. The sections were counterstained with Mayer's Hematoxylin (Sigma) and examined under a Leica microscope. The images were analyzed with the use of ImageScope software (Aperio). Synaptophysin expression was analyzed using the membrane algorithm, LC3 expression was analyzed using the positive pixel algorithm, and nuclear algorithm was used to quantify Ki-67, T-antigen, and AR positive cells.

Transmission electron microscopy

Transmission electron microscopy using prostate tissue was performed for visualization and quantitation of autophagic vacuoles. Transmission electron microscopy was performed essentially as described by us previously (26). Briefly, prostate tissues were immersion fixed in 2.5% electron microscopy grade glutaraldehyde in PBS overnight at 4°C, washed in PBS, and then post-fixed in 1% aqueous osmium tetroxide containing 0.1% potassium ferricyanide for 1 hour. Following three PBS washes, samples were dehydrated through a graded series of 30% to 100% ethanol. Propylene oxide (100%) was then infiltrated in a 1:1 mixture of propylene oxide and Poly/Bed 812 epoxy resin (Epon) (Polysciences) for 1 hour. After several changes of 100% resin over 24 hours, samples were embedded in molds, cured at 37°C overnight, followed by additional hardening at 65°C for 2 days. Ultrathin (60 nm) sections were collected on 200 mesh copper grids, stained with 2% uranyl acetate in 50% methanol for 10 minutes, and then stained in 1% lead citrate for 7 minutes. Sections were imaged using JEOL 1011 transmission electron microscope at 80 kV fitted with a side-mount digital camera.

TUNEL Assay

Prostate sections were deparaffinized, rehydrated, and then used to visualize apoptotic bodies by TUNEL staining. TUNEL staining was performed according to the supplier's instructions. Four to five randomly selected, non-overlapping, and non-necrotic fields were imaged to score TUNEL-positive cells.

Western Blotting

Tumor samples from each group were processed for western blotting as previously described (10). Western blotting was done as described previously (26).

Determination of VEGF Levels

The levels of VEGF in tumor lysates from different groups were measured using a commercially available kit according to the supplier's instructions. The results were normalized to protein concentration.

Plasma proteomics by 2-dimensional gel electrophoresis and mass spectrometry

Plasma proteomics was performed by Applied Biomics. Randomly selected plasma samples (without complete knowledge of the histopathological data) from control mice (n=3), SFN alone-treated mice (n=3), and mice treated with the SFN+CQ combination (n=4) were used

for plasma proteomics analyses essentially as described by us previously (26). Results are expressed as a ratio of abundance of a desired protein in the SFN or SFN+CQ group to control. Cluster analysis for protein abundance changes was performed using a public bioinformatics tool [The Database for Annotation, Visualization and Integrated Discovery (DAVID), http://david.abcc.ncifcrf.gov/home.jsp] (27). The software uses a novel algorithm to measure the relationships among the annotation terms based on the degrees of their co-association genes to group the similar, redundant, and heterogeneous annotation contents from the same or different resources into annotation groups.

Statistical analysis

The association of incidence and treatment was examined by Fisher's exact test. Comparisons of lymph node metastasis or prostate size between the four treatment groups were conducted using Wilcoxon two-sample test. Area of PIN and WDC was analyzed by one-way analysis of variance (ANOVA) with Bonferroni's multiple comparison adjustment. Statistical significance of differences in mechanistic correlates (immunohistochemical analyses, TUNEL-positive apoptotic bodies, and number of autophagic vacuoles) was determined using one-way ANOVA followed by Bonferroni's adjustment. Statistical analyses were performed using SAS version 9.2 or GraphPad Prism version 4.03. Difference was considered significant at P value of < 0.05.

Results

Effects of SFN and/or CQ treatments on PDC

We have shown previously that SFN treatment induces cytoprotective autophagy in cultured human prostate cancer cells (PC-3 and LNCaP) regardless of the AR or p53 status (22). The main objective of the present study was to determine the *in vivo* significance of these observations. We hypothesized that the chemopreventive efficacy of SFN against prostate cancer might be augmented by pharmacological inhibition of autophagy using CQ, which disrupts lysosome acidification (28). As shown in Figure 1A, the initial and final body weights of the mice were not affected by treatments with SFN and/or CQ when compared with control. Wet weight of the prostate is an indicator of tumor burden in the TRAMP model. The mean prostate weight of the mice treated with SFN+CQ (1.43 g) was lower by about 45% compared with control group (P=0.02) (Figure 1B). The mean prostate weight of the mice of SFN+CQ group was also lower compared with SFN alone (2.74 g) or CQ alone group (2.47 g) but the difference did not reach statistical significance (Figure 1B). Microscopic examinations of the whole mount H&E stained sections from the prostate of mice revealed that PDC was the predominant pathology if the mean prostate weight was >1 g. We therefore computed percentage of mice with prostate weight of >1 g. As shown in Figure 1C, the percentage of mice with prostate weight >1 g was significantly lower in the SFN+CQ group (12%) compared with control (50%), CQ alone (44%) and SFN alone group (54%) (Figure 1C). Collectively, these results indicated inhibition of PDC upon co-treatment with SFN and CQ, which was not observed with SFN alone administration.

Effects of SFN and/or CQ treatments on lymph node metastasis

Figure 2A depicts metastatic lymph node in a representative mouse each of the control group and the SFN+CQ treatment group. Lymph node metastasis incidence in the SFN+CQ-treated mice was lower (12%) compared with that of the control group (36%), CQ alone group (36%) or the SFN alone group (36%) (Figure 2B). The size of the metastatic lymph node in the mice of SFN+CQ group was significantly lower (42% lower) compared with the control group (Figure 2C). These results indicated that treatment with SFN+CQ combination was associated with inhibition of lymph node metastasis, which was not observed by treatment with SFN alone.

Analyses of PIN and WDC incidence/burden

Figure 3A shows pathology associated with low-grade PIN (LG PIN), high-grade PIN (HG PIN), and WDC in representative TRAMP mice of the control group. Microscopic analysis of PIN and WDC was performed in prostate of mice with mean prostate weight <1 g because PDC is the predominant pathology in mice with mean prostate weight >1 g. Neither SFN alone nor SFN+CQ combination was able to suppress incidence (Figure 3B) or burden (affected area) (Figure 3C) of LG PIN or HG PIN. On the other hand, consistent with our previous observations (10), SFN treatment alone was able to significantly reduce area (79% decrease compared with control, $P < 0.01$) of WDC compared with control (Figure 3B, C). Furthermore, the area of the WDC in mice treated with SFN+CQ combination was about 69% lower compared with that of control mice ($P < 0.01$) (Figure 3C). Collectively, these results indicated that effect of SFN+CQ combination was not superior to SFN alone with respect to the effect on PIN or WDC incidence and burden.

Effect of SFN and/or CQ treatments on neuroendocrine tumors

A small fraction of cells in the TRAMP tumor exhibit neuroendocrine differentiation (29). Figure 4A depicts synaptophysin-positive cells (a marker for neuroendocrine cells) in a representative mouse of each group. The number of synaptophysin-positive cells was not affected by SFN and/or CQ treatments when compared with control (Figure 4A, bar graph).

SFN treatment caused *in vivo* autophagy

Transmission electron microscopy was performed for visualization and quantitation of autophagic vacuoles in the prostate of control mice and those treated with SFN and/or CQ (Figure 4B). CQ impairs autophagic protein degradation by raising intra-lysosomal pH (28,30,31). CQ treatment leads to accumulation of ineffective autophagosomes, which was also observed in the present study (Figure 4B). It is important to point out that distinction between effective and ineffective autophagic vacuoles is not possible by electron microscopy. Nevertheless, the number of autophagosomes was significantly higher in the prostate of SFN-treated mice compared with control (Figure 4B). Autophagy induction by SFN administration *in vivo* was confirmed by immunohistochemical analysis of LC3, which is a critical protein in autophagic machinery (32). Expression of LC3 was relatively higher in the prostate of mice treated with SFN alone and SFN+CQ compared with control but the difference did not reach statistical significance for SFN alone (Figure 4C). Nevertheless, these observations provided *in vivo* evidence for SFN-induced autophagy.

Analysis of Ki-67 and AR expression and TUNEL positive apoptotic bodies

We raised the question of whether SFN-mediated prevention of prostate cancer in TRAMP model was partly due to suppression of the transgene. Expression of T-antigen was not affected by SFN and/or CQ treatments (Figure 5A). While the expression of Ki-67 (a marker of cell proliferation) was significantly lower in the tumors of SFN alone and SFN+CQ group compared with control as well as CQ alone group (Figure 5B), the AR expression did not differ significantly between groups. The TUNEL positive apoptotic bodies were rare in the prostate of control mice or those treated with CQ (Figure 5D). The number of TUNEL positive apoptotic bodies was increased upon treatment with SFN compared with control. The SFN+CQ combination was even more effective in increasing the number of TUNEL positive cells but the difference was insignificant due to large variability.

We proceeded to determine the expression of p62, which is another marker of autophagy, and caspase-3 cleavage, which is an indicator of apoptosis, using tumor supernatants from 3–4 mice of each group. Two out of four samples showed decreased intensity for p62 expression in the SFN+CQ group when compared with control (Supplementary Figure S1).

Cleavage of caspase-3 was very low in tumors of control and CQ alone groups as expected but was increased in SFN alone and SFN+CQ groups attesting to apoptosis induction by these treatments (Supplementary Figure S1).

Analysis of E-cadherin, vimentin, Atg5, phospho-mTOR, and VEGF proteins

Epithelial-mesenchymal transition (EMT), biochemically characterized by loss of adherens junction protein E-cadherin concomitant with induction of vimentin, is implicated as a significant contributor to prostate cancer progression as well as metastatic spread (33,34). The expression of E-cadherin protein was either un-detectable or very low in the tumors of control, CQ alone, and SFN alone treatment groups. On the other hand, the expression of E-cadherin was clearly visible in tumors of mice from the SFN+CQ treatment group (Figure 6A). Due to large variability in E-cadherin expression and less than sufficient power because of a profound effect of the SFN+CQ combination on prostate cancer development, statistical analysis was not possible (Figure 6B). Nevertheless consistent with the E-cadherin protein expression data, the level of vimentin protein was lower in the tumors of SFN+CQ group in comparison with other groups (Figure 6A). Thus, potential inhibition of EMT in the tumor by the SFN+CQ combination treatment likely contributes to its anti-metastatic effect. Likewise, there was a trend of an increase in protein levels of autophagy regulator Atg5 in the tumors of SFN+CQ-treated mice compared with control or SFN treatment groups (Figure 6A and B). mTOR is another protein implicated in regulation of autophagy (35). Protein level of phospho-mTOR (active form) was relatively lower in the tumors of SFN +CQ-treated mice at least compared with the tumors of control mice. Finally, SFN+CQ combination also resulted in a modest decrease in protein levels of angiogenic cytokine VEGF (36) in the tumor in comparison with those of control and CQ groups of mice. These observations provide mechanistic insights into the chemopreventive effect of the SFN+CQ combination.

Changes in plasma protein abundance upon treatment with SFN and SFN+CQ

The cut-off criteria for spot selection and protein identification were at least 1.3-fold difference (increase or decrease) in abundance of different proteins in the plasma of mice from SFN+CQ group compared with control and P value of ≤ 0.10. Some of the spots meeting these criteria were abundant proteins (eg, hemoglobin, macroglobulin etc.) even though depletion of abundant proteins was performed prior to the 2-dimensional gel electrophoresis. The abundant proteins are not included in Table 1, which summarizes plasma protein abundance changes in response to treatment with SFN alone or SFN+CQ combination in comparison with control. Cluster analysis of the proteomics results indicated significant enrichment of proteins associated with proteasome, protease inhibitor family, and protein-lipid complex (results not shown).

Discussion

Our initial observations of autophagy induction by SFN treatment in cultured prostate cancer cells (22,37) have since been confirmed by other investigators in different types of cancer cells (38–41). Majority of these studies support our conclusions that autophagy is a cytoprotective mechanism (38–40). For example, pharmacological inhibition of autophagy using 3-methyl adenine or bafilomycin A1 augments SFN-induced apoptotic cell death in cultured human colon and breast cancer cells (38,40). However, the *in vivo* significance of these findings was unclear. The present study is the first published report to demonstrate that (a) SFN administration causes *in vivo* autophagy as evidenced by transmission electron microscopy and immunohistochemical analyses of LC3 expression, and (b) inhibition of autophagy by an agent (CQ) already under clinical investigation as a chemotherapy sensitizer (30) increases efficacy of SFN for prevention of prostate cancer reflected by

significant inhibition of PDC by the SFN+CQ combination, which is not observed with SFN treatment alone. These observations merit investigation of the SFN+CQ combination for prevention of prostate cancer in a clinical setting.

We have shown previously that the incidence of metastatic nodules in the lung, but not the lymph node metastasis, is decreased upon treatment with SFN alone (10). In the present study, the overall incidence of lung metastasis in control mice was surprisingly lower (<10%) than observed by us previously (>75%) in TRAMP model (10,42). On the other hand, the overall incidence of lymph node metastasis observed in control mice in the present study was comparable to those reported previously (10,42). The present study reveals that the incidence as well as size of lymph node metastasis is significantly reduced upon treatment with SFN+CQ combination when compared with control group. The mechanism by which SFN+CQ combination suppresses metastasis likely involves inhibition of EMT and suppression of proangiogenic cytokine VEGF. We have shown previously that SFN treatment alone is unable to restore E-cadherin expression (10). Nevertheless, further studies are needed to validate these conclusions with larger sample size, which was not possible in the present study.

The SFN+CQ combination regimen is not superior to SFN alone with respect to inhibition of PIN or WDC. Consistent with our previous observations (10) SFN alone is able to modestly but significantly inhibit WDC incidence and burden. However, effect on WDC incidence is abolished when SFN is combined with CQ. It is possible that SFN+CQ combination is more effective in inducing apoptosis in fully transformed cells (PDC) than in pre-neoplastic cells (eg, PIN). This speculation is consistent with our earlier observations that normal human prostate epithelial cells are resistant to SFN-induced apoptosis (15). Relatively greater abundance of TUNEL-positive apoptotic cells and increased cleavage of caspase-3 in the tumors from mice treated with the SFN+CQ combination compared with SFN alone treatment group (present study) provides added support to this contention.

We have shown previously that SFN treatment causes transcriptional repression of AR in human prostate cancer cells leading to down-regulation of *AR*-regulated gene product prostate-specific antigen (20). The present study reveals that level of AR protein *in vivo* is not decreased upon treatment with SFN alone or SFN+CQ combination. It is possible that a more intense dosing regimen of SFN administration (i.e., daily administration or higher dose) is required to observe suppression of AR protein expression *in vivo.* At the same time, the possibility that SFN-mediated suppression of AR signaling is an *in vitro* phenomenon can't be discarded.

Successful implementation of a cancer chemopreventive strategy is contingent upon systematic investigations starting with cellular studies to identify promising agents and to define the mechanism(s) underlying their cancer protective effect to animal-based studies focusing not only on *in vivo* bio-availability, safety, and efficacy assessments but also on identification of biomarker(s) predictive of tissue exposure, and possibly response, prior to translation in humans with a pilot biomarker modulation trial followed by larger studies with cancer incidence as the primary end point. Identification of suitable biomarker(s) is particularly essential for the clinical development of chemopreventive agents as cancer incidence is too rigorous of an end point for malignancies with long latency such as prostate cancer. Plasma proteomics performed in the present study provides novel leads that can be followed-up to identify biomarkers associated with SFN+CQ exposure/response. Abundance change of some of these proteins seems unique to the SFN+CQ combination. For example, abundance of alpha 1 acid glycoprotein, which is an acute inflammatory biomarker that increases in various conditions including malignancy (43), is decreased after SFN+CQ treatment (2.6-fold decrease compared with control) but its level increases in the plasma of

SFN alone treated mice. We observed decreased abundance of kininogen-1 isoform 1 precursor and transthyretin precursor in the plasma of SFN+CQ-treated mice compared with control. Abundance of these proteins is not altered by SFN administration alone (present study). Interestingly, transthyretin and high-molecular weight kininogen were found to be significantly enhanced in the sera of patients with prostate cancer compared with those of benign prostatic hyperplasia (44).

We found increased abundance of sulfated glycoprotein-2 isoform 2 in the plasma of SFN +CQ-treated mice compared with control. This protein is also known as clusterin and expressed as three forms with different sub-cellular localization (45). Expression of clusterin was shown to be down-regulated during prostate cancer progression in the TRAMP model (46). Mice with homozygous or heterozygous deletion of clusterin exhibited PIN or differentiated carcinoma (47). Crossing of clusterin knockout mice with TRAMP resulted in a strong enhancement of metastatic spread suggesting a tumor suppressor role for clusterin (47). At the same time, some studies have suggested oncogenic function for clusterin (48). Nevertheless, SFN+CQ combination restores plasma level of isoform 2 of clusterin, and this effect is not observed upon treatment with SFN alone.

Men with prostate cancer suffer significant impairments in quality of life not only from the disease itself but also as a consequence of the treatments. Because the commonly associated risk factors for prostate cancer, including age, race, and genetic predisposition are not easily modifiable, novel approaches for prevention of this disease are desirable. Moreover, a clinically viable preventive intervention against prostate cancer is still lacking (49,50). For example, increased incidence of high-grade tumors in the treatment arm in chemoprevention trials with 5-α-reductase inhibitors hindered their broad acceptance as a preventive strategy (49,50). The results of the present study provide pre-clinical *in vivo* evidence for prostate cancer preventive efficacy of a novel and clinically viable combination regimen to warrant investigations in a clinical setting.

Supplementary Material

Refer to Web version on PubMed Central for supplementary material.

Acknowledgments

Grant Support

This work was supported by the grant RO1 CA115498-07 awarded by the National Cancer Institute. This research used the Animal Facility and Tissue and Research Pathology Facility supported in part by a grant from the National Cancer Institute at the National Institutes of Health (P30 CA047904).

References

1. Ambrosone CB, McCann SE, Freudenheim JL, Marshall JR, Zhang Y, Shields PG. Breast cancer risk in premenopausal women is inversely associated with consumption of broccoli, a source of isothiocyanates, but is not modified by GST genotype. J Nutr. 2004; 134:1134–8. [PubMed: 15113959]
2. Kolonel LN, Hankin JH, Whittemore AS, Wu AH, Gallagher RP, Wilkens LR, et al. Vegetables, fruits, legumes and prostate cancer: a multiethnic case-control study. Cancer Epidemiol Biomarkers Prev. 2000; 9:795–804. [PubMed: 10952096]
3. Siegel R, Naishadham D, Jemal A. Cancer statistics, 2012. CA Cancer J Clin. 2012; 62:10–29. [PubMed: 22237781]
4. Fahey JW, Zalcmann AT, Talalay P. The chemical diversity and distribution of glucosinolates and isothiocyanates among plants. Phytochemistry. 2001; 56:5–51. [PubMed: 11198818]

5. Singh SV, Singh K. Cancer chemoprevention with dietary isothiocyanates mature for clinical translational research. Carcinogenesis. 2012; 33:1833–42. [PubMed: 22739026]
6. Zhang Y, Kensler TW, Cho CG, Posner GH, Talalay P. Anticarcinogenic activities of sulforaphane and structurally related synthetic norbornyl isothiocyanates. Proc Natl Acad Sci USA. 1994; 91:3147–50. [PubMed: 8159717]
7. Conaway CC, Wang CX, Pittman B, Yang YM, Schwartz JE, Tian D, et al. Phenethyl isothiocyanate and sulforaphane and their *N*-acetylcysteine conjugates inhibit malignant progression of lung adenomas induced by tobacco carcinogens in A/J mice. Cancer Res. 2005; 65:8548–57. [PubMed: 16166336]
8. Fahey JW, Haristoy X, Dolan PM, Kensler TW, Scholtus I, Stephenson KK, et al. Sulforaphane inhibits extracellular, intracellular, and antibiotic-resistant strains of *Helicobacter pylori* and prevents benzo[*a*]pyrene-induced stomach tumors. Proc Natl Acad Sci USA. 2002; 99:7610–5. [PubMed: 12032331]
9. Chung FL, Conaway CC, Rao CV, Reddy BS. Chemoprevention of colonic aberrant crypt foci in Fischer rats by sulforaphane and phenethyl isothiocyanate. Carcinogenesis. 2000; 21:2287–91. [PubMed: 11133820]
10. Singh SV, Warin R, Xiao D, Powolny AA, Stan SD, Arlotti JA, et al. Sulforaphane inhibits prostate carcinogenesis and pulmonary metastasis in TRAMP mice in association with increased cytotoxicity of natural killer cells. Cancer Res. 2009; 69:2117–25. [PubMed: 19223537]
11. Keum YS, Khor TO, Lin W, Shen G, Kwon KH, Barve A, et al. Pharmacokinetics and pharmacodynamics of broccoli sprouts on the suppression of prostate cancer in transgenic adenocarcinoma of mouse prostate (TRAMP) mice: implication of induction of Nrf2, HO-1 and apoptosis and the suppression of Akt-dependent kinase pathway. Pharm Res. 2009; 26:2324–31. [PubMed: 19669099]
12. Singh AV, Xiao D, Lew KL, Dhir R, Singh SV. Sulforaphane induces caspase-mediated apoptosis in cultured PC-3 human prostate cancer cells and retards growth of PC-3 xenografts *in vivo*. Carcinogenesis. 2004; 25:83–90. [PubMed: 14514658]
13. Singh SV, Herman-Antosiewicz A, Singh AV, Lew KL, Srivastava SK, Kamath R, et al. Sulforaphane-induced G_2/M phase cell cycle arrest involves checkpoint kinase 2-mediated phosphorylation of cell division cycle 25C. J Biol Chem. 2004; 279:25813–22. [PubMed: 15073169]
14. Singh SV, Srivastava SK, Choi S, Lew KL, Antosiewicz J, Xiao D, et al. Sulforaphane-induced cell death in human prostate cancer cells is initiated by reactive oxygen species. J Biol Chem. 2005; 280:19911–24. [PubMed: 15764812]
15. Choi S, Singh SV. Bax and Bak are required for apoptosis induction by sulforaphane, a cruciferous vegetable-derived cancer chemopreventive agent. Cancer Res. 2005; 65:2035–43. [PubMed: 15753404]
16. Bertl E, Bartsch H, Gerhäuser C. Inhibition of angiogenesis and endothelial cell functions are novel sulforaphane-mediated mechanisms in chemoprevention. Mol Cancer Ther. 2006; 5:575–85. [PubMed: 16546971]
17. Myzak MC, Karplus PA, Chung FL, Dashwood RH. A novel mechanism of chemoprotection by sulforaphane: inhibition of histone deacetylase. Cancer Res. 2004; 64:5767–74. [PubMed: 15313918]
18. Xu C, Shen G, Chen C, Gélinas C, Kong AN. Suppression of NF-κB and NF-κB-regulated gene expression by sulforaphane and PEITC through IκBα, IKK pathway in human prostate cancer PC-3 cells. Oncogene. 2005; 24:4486–95. [PubMed: 15856023]
19. Hahm ER, Singh SV. Sulforaphane inhibits constitutive and interleukin-6-induced activation of signal transducer and activator of transcription 3 in prostate cancer cells. Cancer Prev Res. 2010; 3:484–94.
20. Kim SH, Singh SV. D,L-Sulforaphane causes transcriptional repression of androgen receptor in human prostate cancer cells. Mol Cancer Ther. 2009; 8:1946–54. [PubMed: 19584240]
21. Surh YJ. Cancer chemoprevention with dietary phytochemicals. Nat Rev Cancer. 2003; 3:768–80. [PubMed: 14570043]

22. Herman-Antosiewicz A, Johnson DE, Singh SV. Sulforaphane causes autophagy to inhibit release of cytochrome *c* and apoptosis in human prostate cancer cells. Cancer Res. 2006; 66:5828–35. [PubMed: 16740722]
23. Dikic I, Johansen T, Kirkin V. Selective autophagy in cancer development and therapy. Cancer Res. 2010; 70:3431–4. [PubMed: 20424122]
24. Kondo Y, Kanzawa T, Sawaya R, Kondo S. The role of autophagy in cancer development and response to therapy. Nat Rev Cancer. 2005; 5:726–34. [PubMed: 16148885]
25. Greenberg NM, DeMayo F, Finegold MJ, Medina D, Tilley WD, Aspinall JO, et al. Prostate cancer in a transgenic mouse. Proc Natl Acad Sci USA. 1995; 92:3439–43. [PubMed: 7724580]
26. Powolny AA, Bommareddy A, Hahm ER, Normolle DP, Beumer JH, Nelson JB, et al. Chemopreventative potential of the cruciferous vegetable constituent phenethyl isothiocyanate in a mouse model of prostate cancer. J Natl Cancer Inst. 2011; 103:571–84. [PubMed: 21330634]
27. Huang DW, Sherman BT, Lempicki RA. Systematic and integrative analysis of large gene lists using DAVID bioinformatics resources. Nat Protoc. 2009; 4:44–57. [PubMed: 19131956]
28. Michihara A, Toda K, Kubo T, Fujiwara Y, Akasaki K, Tsuji H. Disruptive effect of chloroquine on lysosomes in cultured rat hepatocytes. Biol Pharm Bull. 2005; 28:947–51. [PubMed: 15930724]
29. Chiaverotti T, Couto SS, Donjacour A, Mao JH, Nagase H, Cardiff RD, et al. Dissociation of epithelial and neuroendocrine carcinoma lineages in the transgenic adenocarcinoma of mouse prostate model of prostate cancer. Am J Pathol. 2008; 172:236–46. [PubMed: 18156212]
30. Hu YL, Jahangiri A, DeLay M, Aghi MK. Tumor cell autophagy as an adaptive response mediating resistance to treatments such as antiangiogenic therapy. Cancer Res. 2012; 72:4294–9. [PubMed: 22915758]
31. Amaravadi RK, Yu D, Lum JJ, Bui T, Christophorou MA, Evan GI, et al. Autophagy inhibition enhances therapy-induced apoptosis in a *Myc*-induced model of lymphoma. J Clin Invest. 2007; 117:326–36. [PubMed: 17235397]
32. Kabeya Y, Mizushima N, Ueno T, Yamamoto A, Kirisako T, Noda T, et al. LC3, a mammalian homologue of yeast Apg8p, is localized in autophagosome membranes after processing. EMBO J. 2000; 19:5720–8. [PubMed: 11060023]
33. Thiery JP. Epithelial-mesenchymal transitions in tumour progression. Nat Rev Cancer. 2002; 2:442–54. [PubMed: 12189386]
34. Hugo H, Ackland ML, Blick T, Lawrence MG, Clements JA, Williams ED, et al. Epithelial-mesenchymal and mesenchymal-epithelial transitions in carcinoma progression. J Cell Physiol. 2007; 213:374–83. [PubMed: 17680632]
35. Pyo JO, Nah J, Jung YK. Molecules and their functions in autophagy. Exp Mol Med. 2012; 44:73–80. [PubMed: 22257882]
36. McMahon G. VEGF receptor signaling in tumor angiogenesis. Oncologist. 2000; 5(Suppl 1):3–10. [PubMed: 10804084]
37. Xiao D, Powolny AA, Antosiewicz J, Hahm ER, Bommareddy A, Zeng Y, et al. Cellular responses to cancer chemopreventive agent D,L-sulforaphane in human prostate cancer cells are initiated by mitochondrial reactive oxygen species. Pharm Res. 2009; 26:1729–38. [PubMed: 19384467]
38. Nishikawa T, Tsuno NH, Okaji Y, Shuno Y, Sasaki K, Hongo K, et al. Inhibition of autophagy potentiates sulforaphane-induced apoptosis in human colon cancer cells. Ann Surg Oncol. 2010; 17:592–602. [PubMed: 19830499]
39. Jeong HS, Choi HY, Lee ER, Kim JH, Jeon K, Lee HJ, et al. Involvement of caspase-9 in autophagy-mediated cell survival pathway. Biochim Biophys Acta. 2011; 1813:80–90. [PubMed: 20888374]
40. Kanematsu S, Uehara N, Miki H, Yoshizawa K, Kawanaka A, Yuri T, et al. Autophagy inhibition enhances sulforaphane-induced apoptosis in human breast cancer cells. Anticancer Res. 2010; 30:3381–90. [PubMed: 20944112]
41. Naumann P, Fortunato F, Zentgraf H, Büchler MW, Herr I, Werner J. Autophagy and cell death signaling following dietary sulforaphane act independently of each other and require oxidative stress in pancreatic cancer. Int J Oncol. 2011; 39:101–9. [PubMed: 21537844]

42. Singh SV, Powolny AA, Stan SD, Xiao D, Arlotti JA, Warin R, et al. Garlic constituent diallyl trisulfide prevents development of poorly differentiated prostate cancer and pulmonary metastasis multiplicity in TRAMP mice. Cancer Res. 2008; 68:9503–11. [PubMed: 19010926]
43. Kanoh Y, Ohtani H, Egawa S, Baba S, Akahoshi T. Levels of acute inflammatory biomarkers in advanced prostate cancer patients with α_2-macroglobulin deficiency. Int J Oncol. 2011; 39:1553–8. [PubMed: 21894431]
44. Jayapalan JJ, Ng KL, Razack AH, Hashim OH. Identification of potential complementary serum biomarkers to differentiate prostate cancer from benign prostatic hyperplasia using gel- and lectin-based proteomics analyses. Electrophoresis. 2012; 33:1855–62. [PubMed: 22740474]
45. Rizzi F, Bettuzzi S. The clusterin paradigm in prostate and breast carcinogenesis. Endocr Relat Cancer. 2010; 17:R1–17. [PubMed: 19903745]
46. Caporali A, Davalli P, Astancolle S, D'Arca D, Brausi M, Bettuzzi S, et al. The chemopreventive action of catechins in the TRAMP mouse model of prostate carcinogenesis is accompanied by clusterin over-expression. Carcinogenesis. 2004; 25:2217–24. [PubMed: 15358631]
47. Bettuzzi S, Davalli P, Davoli S, Chayka O, Rizzi F, Belloni L, et al. Genetic inactivation of ApoJ/clusterin: effects on prostate tumourigenesis and metastatic spread. Oncogene. 2009; 28:4344–52. [PubMed: 19784068]
48. Miyake H, Muramaki M, Kurahashi T, Yamanaka K, Hara I, Gleave M, et al. Expression of clusterin in prostate cancer correlates with Gleason score but not with prognosis in patients undergoing radical prostatectomy without neoadjuvant hormonal therapy. Urology. 2006; 68:609–14. [PubMed: 16979705]
49. Thompson IM, Goodman PJ, Tangen CM, Lucia MS, Miller GJ, Ford LG, et al. The influence of finasteride on the development of prostate cancer. N Engl J Med. 2003; 349:215–24. [PubMed: 12824459]
50. Andriole GL, Bostwick DG, Brawley OW, Gomella LG, Marberger M, Montorsi F, et al. Effect of dutasteride on the risk of prostate cancer. N Engl J Med. 2010; 362:1192–202. [PubMed: 20357281]

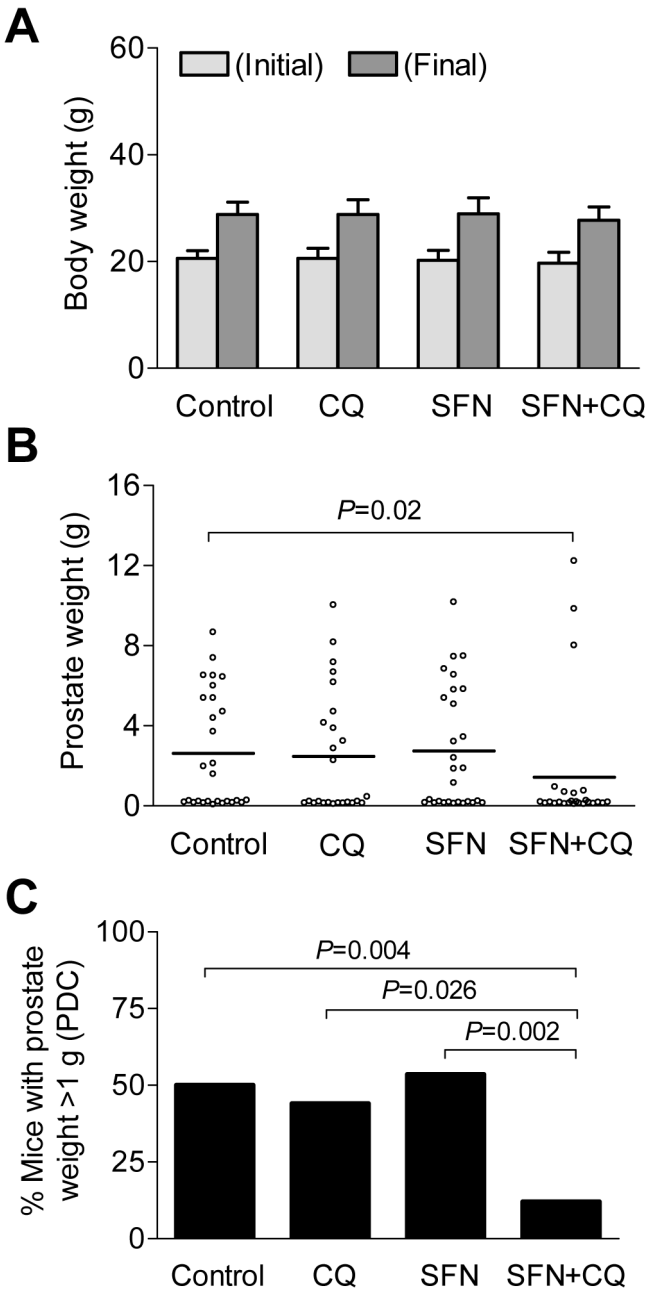

Figure 1.

D,L-Sulforaphane (SFN) and chloroquine (CQ) combination treatment decreases prostate weight in TRAMP mice. (A) Initial and final body weights and (B) mean wet prostate weights in mice of control group (n=28), CQ alone group (n=25), SFN alone group (n=28) and SFN+CQ group (n=25). Results shown are mean ± SD. Statistical significance for data in panel B was determined by Wilcoxon two-sample test. (C) Percentage of mice with mean prostate weight of >1 g. Statistical significance was determined by Fisher's exact test.

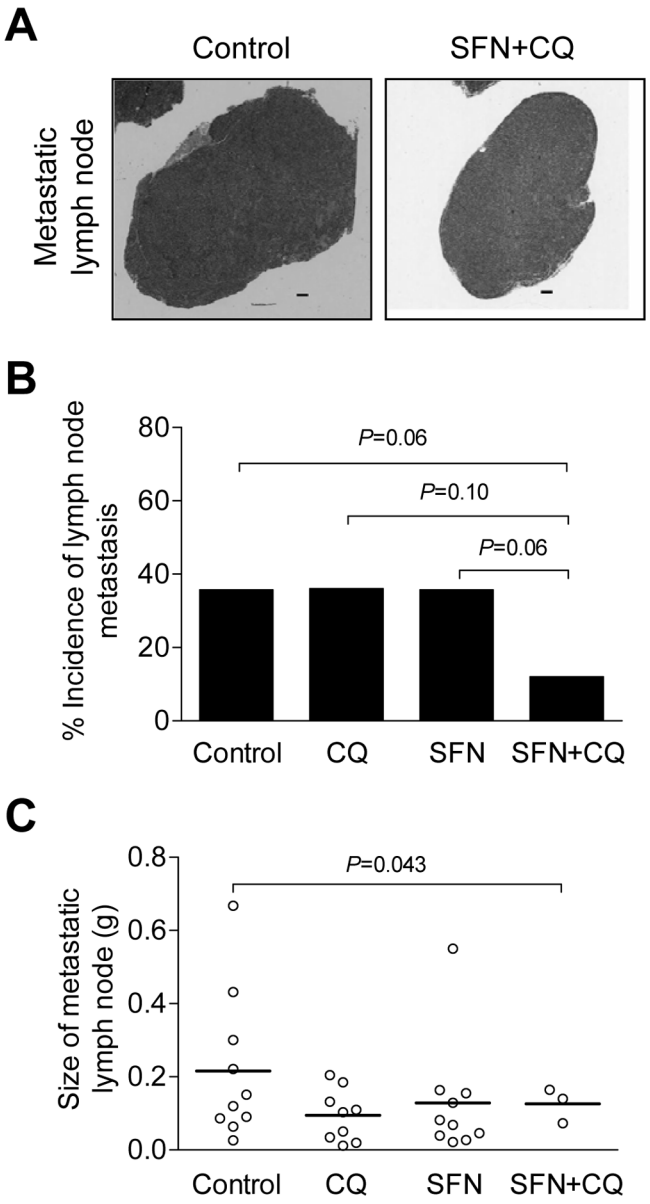

Figure 2.

D,L-Sulforaphane (SFN) and chloroquine (CQ) combination treatment decreases lymph node metastasis in TRAMP mice. (A) Microscopic images depicting lymph node metastasis in a representative mouse each of the control group and the SFN+CQ group (magnification ×5, scale bar- 400 μm). (B) Percentage of mice with lymph node metastasis. Statistical significance was determined by Fisher's exact test. (C) Size of lymph node metastasis in mice of control group (n=10), CQ alone group (n=9), SFN alone group (n=10), and SFN +CQ group (n=3). Results shown are mean ± SD. Statistical significance was determined by Wilcoxon two-sample test.

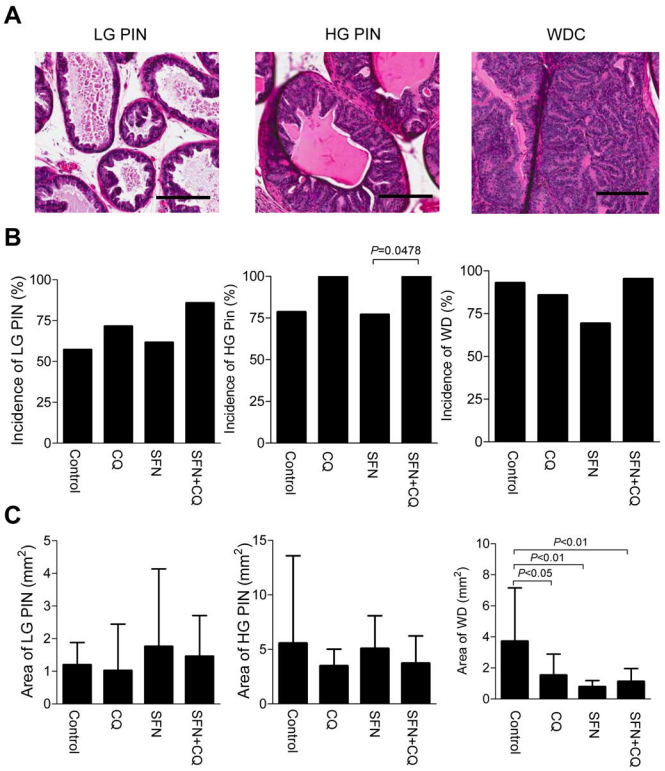

Figure 3.

Effects of D,L-sulforaphane (SFN) and/or chloroquine (CQ) treatments on incidence and burden (affected area) of low-grade prostatic intraepithelial neoplasia (LG PIN), high-grade PIN (HG PIN), and well-differentiated prostate cancer (WDC) in TRAMP mice. (A) Microscopic images depicting pathology associated with LG PIN, HG PIN, and WDC (magnification ×200, scale bar- 50 μm). (B) Incidence of LG PIN, HG PIN, and WDC in the prostate of control mice and those treated with SFN and/or CQ. Statistical significance was determined by Fisher's exact test. (C) Area of LG PIN, HG PIN, and WDC in the prostate of mice from the control group (n=13), CQ alone group (n=12), SFN alone group (n=9), and SFN+CQ group (n=20). Results shown are mean ± SD. Statistical significance was determined by one-way ANOVA followed by Bonferroni's multiple comparison test.

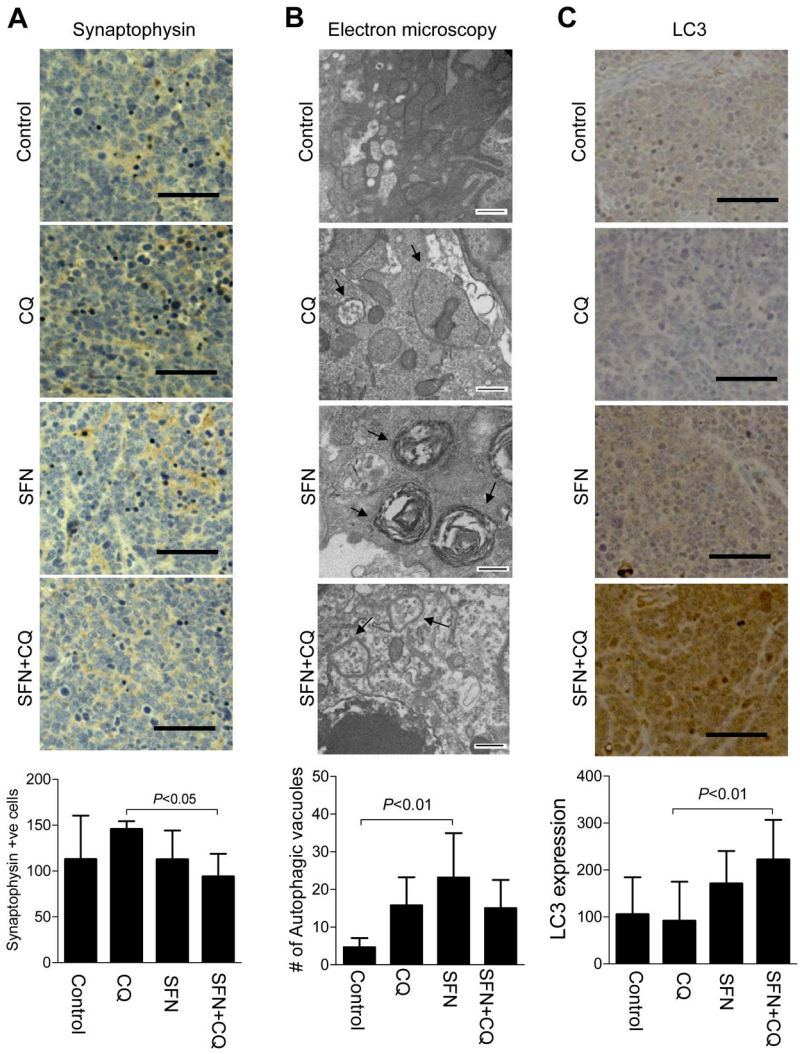

Figure 4.

Effects of D,L-sulforaphane (SFN) and/or chloroquine (CQ) treatments on (A) synaptophysin expression (magnification ×200, scale bar- 50 μm), (B) autophagic vacuoles quantified from transmission electron micrographs (magnification ×25,000, scale bar- 500 nm), and (C) LC3 expression (magnification ×200, scale bar- 50 μm) in the prostate of TRAMP mice. Results shown are mean ± SD (n=7 for each group in panels A and C). For quantitation of autophagic vacuoles, prostate tissues from 2 mice of each group were used for transmission electron microscopy, and entire fields from 3–6 sections for each sample were examined for presence of autophagosomes. Results shown in panel B are mean ± SD (n=6–9). Statistical significance was determined by one-way ANOVA followed by Bonferroni's multiple comparison test.

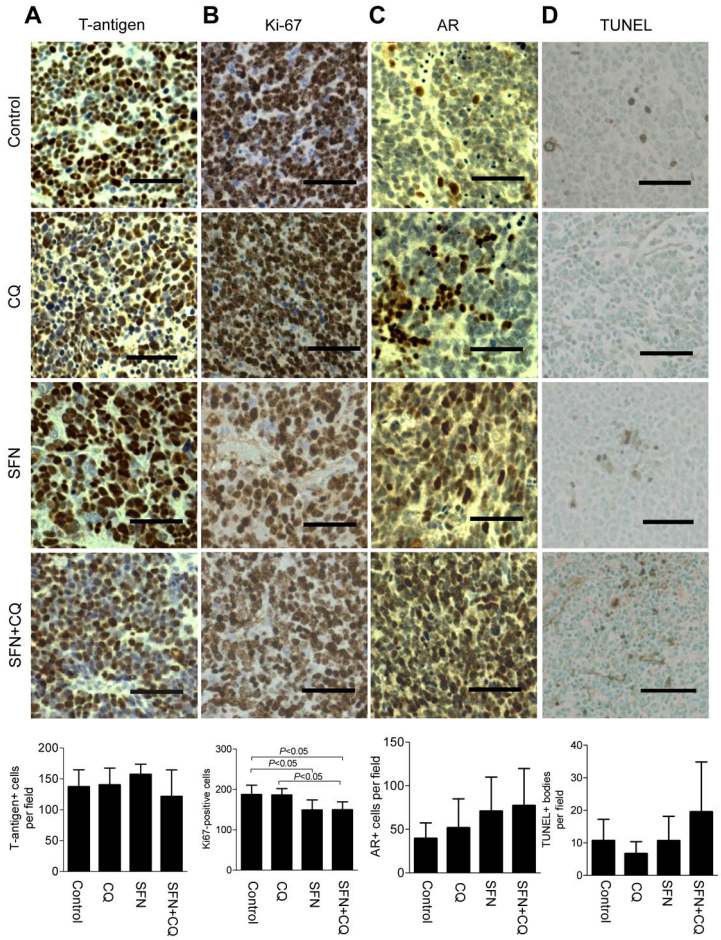

Figure 5.

Effects of D,L-sulforaphane (SFN) and/or chloroquine (CQ) treatments on T-antigen expression (A) T-antigen expression (magnification ×200, scale bar- 50 μm), (B) Ki-67 expression (magnification ×200, scale bar- 50 μm), (C) AR expression (magnification ×200, scale bar- 50 μm), and (D) TUNEL-positive apoptotic bodies in the prostate of TRAMP mice. Results shown are mean ± SD (n=7 for each group). Statistical significance was determined by one-way ANOVA followed by Bonferroni's multiple comparison test.

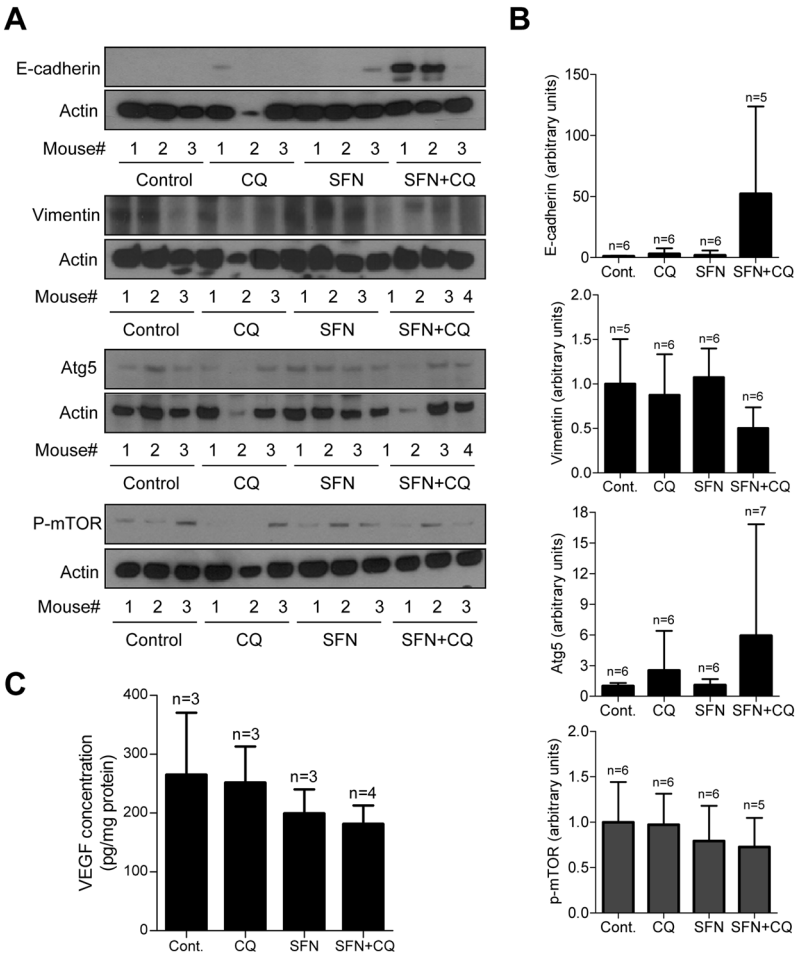

Figure 6.

Effects of D,L-sulforaphane (SFN) and/or chloroquine (CQ) treatments on E-cadherin, vimentin, Atg5, phospho-mTOR, and VEGF protein levels. (A) Western blotting for E-cadherin, vimentin, Atg5, and phospho-mTOR using tumor lysates from mice of the control group (n=5–6), and those treated with SFN alone (n=6), CQ alone (n=6), and SFN+CQ combination (n=5–7). (B) Quantitation of the western blotting data. (C) Levels of VEGF in tumor lysates from mice of the control group and those treated with SFN and/or CQ.

Table 1

Plasma proteins altered by SFN or SFN+CQ administration in TRAMP mice

Protein Name	Master No.	SFN/control		SFN+CQ/control	
		P value	Ratio	*P* value	Ratio
Serine (or cysteine) peptidase inhibitor, clade A, member 3K [Mus musculus]	83	0.600	1.1	0.062	−1.3
Hemopexin precursor [Mus musculus]	195	0.590	−1.1	0.035	−1.5
Transferrin [Mus musculus]	201	0.620	−1.1	0.021	−1.4
Hemopexin, partial [Mus musculus]	212	0.500	1.2	0.073	−1.4
Transferrin	229	0.950	1.0	0.093	−1.3
Kininogen-1 isoform 1 precursor [Mus musculus]	277	0.850	1.0	0.031	−1.3
Alpha-1-acid glycoprotein 1 precursor [Mus musculus]	529	0.640	1.7	0.049	−2.6
Apolipoprotein A-IV precursor [Mus musculus]	561	0.760	1.0	0.031	−1.3
Serpina1c protein [Mus musculus]	766	0.960	1.0	0.077	1.6
Sulfated glycoprotein-2 isoform 2 [Mus musculus]	860	0.440	1.2	0.051	1.7
Proteasome subunit alpha type-1 [Mus musculus]	929	0.780	1.0	0.011	−1.7
Transthyretin precursor [Mus musculus]	989	0.500	−1.2	0.004	−2.0
Unnamed protein product [Mus musculus]	1074	0.760	1.1	0.047	−1.8
Proteasome subunit alpha type-4 [Mus musculus]	1033	0.740	1.1	0.090	1.9
Spermatogenesis-associated protein 22 OS=Mus musculus GN=Spata22 PE=2 SV=1	1070	0.350	−1.3	0.006	−2.4
Proteasome subunit alpha type-6 [Mus musculus]	1096	0.250	−1.4	0.008	−2.0
Transthyretin precursor [Mus musculus]	1592	0.980	1.0	0.090	−1.8
Transthyretin precursor [Mus musculus]	1667	0.850	1.0	0.083	−1.6
Transthyretin precursor [Mus musculus]	1687	0.410	1.1	0.016	1.3
Chain A, Crystal Structure Of Mouse Transthyretin	2134	0.100	−1.1	0.100	1.8
Apolipoprotein A-II precursor [Mus musculus]	2383	0.520	1.2	0.079	1.3
Apolipoprotein A-II precursor [Mus musculus]	2435	0.270	1.2	0.003	1.4